



Penerbit ITB

Jl. Ganesa No. 10 Bandung 40132, Indonesia
Telp. 022 - 2504257, Fax. 022 - 2534155
e-mail: itbpress@penerbit.itb.ac.id
web: www.penerbit.itb.ac.id
e-book: itb.bookstore

ISBN 978-602-7861-73-2



PROCEEDINGS OF

ARMS 9
Bali 2016
9th ASIAN ROCK
MECHANICS SYMPOSIUM

PROCEEDINGS OF



9th ASIAN ROCK
MECHANICS SYMPOSIUM

"Harmonizing Rock Mechanics with Sustainable Economic Development"

The Stones Hotel - Bali, A Marriott Autograph Collection Hotel
October 18th - 20th, 2016



TABLE OF CONTENT

Paper Code		Paper Title & Authors	Page
1	KL-1	<i>Standardization of Rock Testing Within The Context of The ISRM Suggested Methods, Associated Practical Issues and Future</i> Prof. Resat Ulusay	KL-1-1
2	KL-2	<i>Prediction of Rock Cutting Performance</i> Prof. Seokwon Jeon	KL-2-1
3	KL-3	<i>Ground Support Design for Sudden and Violent Failures in Hard Rock Tunnels</i> Prof. Ernesto Villaescusa	KL-3-1
4	KL-4	<i>Displacement Monitoring and Assessment of The Stability of Underground Structures</i> Prof. Norikazu Shimizu	KL-4-1
5	KL-5	<i>The Most Important and Influential Factors in Field Measurements in Geomechanics</i> Prof. Shunsuke Sakurai	KL-5-1
6	KL-6	<i>Issues on Rock Dynamics and Future Directions</i> Prof. Ömer Aydan	KL-6-1
7	KL-7	<i>Strength Criteria to The Dynamic Strength of Brittle Rock</i> Prof. Jian Zhao	KL-7-1
8	KL-8	<i>Recent Developments on Rock Mass Stability Investigations Associated with Surface and Underground Excavations in Three Dimensions</i> Prof. Pinnaduwa H. S. W. Kulatilake	KL-8-1
9	KL-9	<i>Role of Geomechanics in Mining Development in Tropical Region</i> Dr. Suseno Kramadibrata	KL-9-1
Oral Presentation			
1	EN1-P60	<i>A Rock Mechanical Model for Overbalanced, Managed Pressure, and Underbalanced Drilling Applications</i> M. N. J. Al Awad	1
2	EN2-P69	<i>Physical Changes of Coal-bearing Rock in the Dumping Site with the Utilization of Fly Ash and Organic Material as Cover Layer to Prevent Acid Mine Drainage Generation</i> S. Dwiki, H. Shimada, R. S. Gautama, T. Sasaoka, G. J. Kusuma	11
3	EN3-P127	<i>Utilization of X-Ray CT Scanning technique in Rock Mechanics Applications</i> Ö. Aydan , N. Tokashiki and M. Edahiro	21
4	EN4-P176	<i>Improved Characterization of Carbonates Capillary Pressure Transition Zones for Optimizing Oil Recovery</i> A. A. Jebbouri and H. A. Belhaj	31
5	IN1-P20	<i>Effect of Dominating Geological Discontinuity on the Seismic Performance of Underground Rock Caverns: A Case Study of Baihetan 1# surge chamber</i> C. Zhen, S. Qian and L. Xianlun	41
6	IN2-P233	<i>Deformation and Strain Measurement of Geo-materials using Extended Digital Image Correlation Technique</i> S. Bhattacharjee and D. Deb	51

7	IN3-P84	<i>Statistical Analysis of Ground Loss Ratio Duo to Large-diameter Shield Tunnel Construction in China</i> C. Wu and Z. Zhu	61
8	IN4-P123	<i>Unlined/Shotcrete Lined Pressure Tunnel Passing Through Himalayan Rock Mass – Design Review of Upper Tamakoshi Headrace Tunnel, Nepal</i> C. B. Basnet and K. K. Panthi	71
9	RMC1-P1	<i>High Strain Rate Characterization of Himalayan Limestone</i> H. Meena, S. Mishra, T. Chakraborty, V. Matsagar, P. Chandel, V. Mangla and M. Singh	81
10	RMC2-P21	<i>Experimental Study of Propagation of 3D Flaws under Static and Dynamic Loading Conditions with the Application of 3D Printing</i> T. Zhou and J.B. Zhu	89
11	RMC3-P86	<i>Strength Reinforcement of Sand Test Specimens Cemented with Calcium Phosphate Compounds and Different Powders</i> R.A.N. Dilrukshi and S. Kawasaki	97
12	RMC4-P174	<i>The Effect of Clay Content on the Strength of Clay-Bearing Rocks</i> S. Kahraman, A. S. Aloglu, B. Aydin and E. Saygin	105
13	RMC5-P194	<i>Geostatistical Study of the Direct Uniaxial Compressive Strength of the Kadilar Marble Quarry</i> Y. Özçelik, F. Atalay and K. Aksoy	111
14	RMC6-P202	<i>Performance Assessment of Fly Ash-mixed Cement Borehole Plugs in Sandstone</i> M. Chiangmai and P. Tepnarong	119
15	CMNM1-P114	<i>Numerical Simulation of Dynamic Semi-Circular Bend Flexure Tests of Rocks Using Split Hopkinson Pressure Bar</i> F. Dai, Y. Xu, T. Zhao and N. W. Xu	127
16	CMNM2-P115	<i>Experimental and Numerical Study on Rock Fracture Toughness Testing Using Cracked Chevron Notched Semi-Circular Bend Specimen</i> M.D. Wei, F. Dai, N.W. Xu, and T. Zhao	137
17	CMNM3-P120	<i>A New Empirical Failure Criterion for Coal Masses at the 3-D level</i> PF. He, P. H.S.W. Kulatilake, DQ. Liu and MC. He	147
18	CMNM4-P49	<i>Numerical Accuracy and Performance of a Particle Integration Scheme for Manifold Method</i> L. Sun, G. F. Han, X. Q. Wang, J. M. Li, X. D. Liu, and X. Jin	157
19	CMNM5-P185	<i>A Coupled FEM-SPH Procedure for the Simulation of Blast Induced Rock Damage</i> A. Khan and D. Deb	167
20	CMNM6-P35	<i>Evaluation of Ground Support by Rock Mass Index and Finite Element Method Numerical Modelling PT Cibaliung Sumberdaya Banten</i> A. Adhareza, S. Saptono and B. D. Nagara	177
21	RE1-P119	<i>A Conceptual Study for Development of 3D Rock Fragmentation Analysis System with Stereo-photogrammetry Technologies</i> R. Degawa, H. Jang, Y. Kawamura, I. Kitahara, E. Topal and Y. Endo	187
22	RE2-P173	<i>Predicting The Performance of an Axial Type Roadheader in Mine Roadway Excavation from The Needle Penetration Index</i> S. Kahraman, A. S. Aloglu, B. Aydin and E. Saygin	195

23	RE3-P19	<i>Characteristics of Rock Blast Damage and Damage Criterion of Limestone Rock Mass</i> S. Wahyudi, H. Shimada, T. Sasaoka, G. M. Simangunsong and Y. Takahashi	203
24	RE4-P14	<i>Variation in the Reactivity of Chemical Solutions on Rock Properties with Changes in Temperature</i> V. Yuan and P. C. Hagan	211
25	RE5-P83	<i>Study on Effect of High Precision Detonation on Fracture Mechanism in Small Scale Blasting Tests</i> Y. Takahashi, T. Saburi, T. Sasaoka, W. Sugeng, H. Shimada and Yuji Ogata	221
26	RE6-P142	<i>Development of a Small Scaled Linear Cutting Machine and Rock Cutting Tests Using Conical Picks</i> HY. Jeong and S. Jeon	229
27	UMOS1-P8	<i>Effects of Carnallite Contents on Stability and Extraction Ratio of Potash Mine</i> A. Luangthip, S. Khamrat and K. Fuenkajorn	239
28	UMOS2-P23	<i>Maximum Unsupported Span and Standup Time of Potash Mine Roof as Affected by Carnallite Contents</i> M. Chobsranoi and K. Fuenkajorn	247
29	UMOS4-P55	<i>Determination of Safe Withdrawal Rates of Compressed-air Energy Storage Caverns in Maha Sarakham Salt</i> T. Thongprapha, S. Khamrat and K. Fuenkajorn	255
30	UMOS3-P42	<i>Study of Displacement Distribution Around Circular Opening Affected by Presence of Discontinuities Using Laboratory Biaxial Test</i> N. F. Qaidahiyani and N. P. Widodo	265
31	UMOS5-P22	<i>Determination of Time-Dependent Strengths of Salt Pillars using Strain Energy Density Criterion</i> P. Junthong and K. Fuenkajorn	275
32	UMOS6-P183	<i>Inorganic Silicate Capsules for Anchoring in the Mines</i> B. P. Khassen, S. N. Lis and R. A. Musin	283
33	EN5-P78	<i>Shear Behavior of Heat-treated Fractures in Beishan Granite</i> Z. Zhao, D. Zhou and H. Pu	289
34	EN6-P192	<i>Critical Reynolds Number for Nonlinear Flow Through Single Fractures: The Roles of Aperture and Surface Roughness</i> R. Liu and Y. Jiang	297
35	EN7-P175	<i>Strength and Permeability of Carbonate Reservoir Rocks</i> P. A. Nawrocki and A. A. Jebbouri	303
36	EN8-P45	<i>Investigation into Evolution of Shale Gas Permeability during the Gas Reservoir Recovery Process</i> P. Cao, J. Liu and YK. Leong	313
37	IN5-P160	<i>Suggestion of Hydraulic Stimulation Guideline Considering Management of Induced Seismicity for Pohang EGS Project</i> KI. Kim, KY. Kim and KB. Min	323
38	IN6-P209	<i>Dynamic Response of Weathered Sandstone with Respect to Physical and Mechanical Characteristics</i> M. M. Mohd-Nordin, M. K. A. Ismail, A. S. Md. Hasan and Z. Mohamed	331
39	IN7-P41	<i>Real-time Monitoring of Tunnel Face Extrusion for Ground Control</i> K. Date, Y. Yokota, Y. Koizumi, T. Yamamoto and F. Uehan	341

40	IN8-P134	<i>Effects of Forepoling Pre-Support Design Parameters on Shallow Tunnel Crown Stability in Weathered Granite</i> R. A. Abdullah, S. M. Yahya, M. A. M. Ismail and H. Mohamad	347
41	RE7-P104	<i>Study on Mechanism and Occurrence Conditions of Fly Rock at Bench Blasting</i> T. Sasaoka, Y. Takahashi, K. Yamaguchi, S. Wahyudi, H. Shimada, T. Saburi and S. Kubota	355
42	RE8-P87	<i>Strain Rate Effect on the Crack Initiation Stress Level under Uniaxial Compression</i> Y. Wicaksana and S. Jeon	365
43	RE9-P15	<i>Effect of Cutter Tool Angle on Rock Cutting Performance</i> K. Rashidi and P. C. Hagan	375
44	RE10-P71	<i>A Case Study on Shield TBM Driving across the Riverbed of the Hangang (River)</i> CS. Kim and JY. Kim	383
45	RE11-P126	<i>Preliminary Rock Engineering Assessment of the Planned Salang Tunnels (Afghanistan)</i> N. Malistani and Ö. Aydan	391
46	RE12-P68	<i>Numerical Waveform Estimation for Vibration and Noise Based on Accurate Delay Time Control Tunnel Blasting</i> K. Iwano, T. Inuzuka, J. Nagae, K. Fukui and K. Hasiba	401
47	CMNM7-P113	<i>DEM Simulation of Cracked Chevron Notched Brazilian Disc Rock Specimen: Fracture Toughness Determination Incorporating Realistic Crack Profiles</i> Y. Xu, F. Dai, N.W. Xu and T. Zhao	411
48	CMNM8-P27	<i>Evaluation of Constitutive Model by the Triaxial Compression Test and the Numerical Analysis Introduced Strain Hardening and Softening</i> Y. Aono, T. Okuno, A. Nakaya and T. Nishi	421
49	CMNM9-P79	<i>Modeling Stress-Induced Failure for Deep Tunnel Excavation of Pahang-Selangor Raw Water Transfer Project</i> R. Azit and M. A. M. Ismail	431
50	CMNM10-P46	<i>Numerical Simulation of Percussive Rock Drilling and Its Modification in Bit Penetration</i> K. Hashiba, K. Fukui, Y. Z. Liang, M. Koizumi and T. Matsuda	441
51	CMNM11-P29	<i>Theoretical Model Using Two Kinds of Function for Distribution of Applied Load in Brazilian Test</i> T. Tsutsumi, R. A. Abdullah and M. F. M. Amin	449
52	CMNM12-P150	<i>Age-Dependent Shotcrete Behavior in Convergence Confinement Method and 3D Numerical Analysis</i> T. Bhandari and M. Kastner	455
53	RMC7-P228	<i>Applicability of Powder-Based 3D Printer in Rock Mechanics</i> S. Fereshtenejad and J. J. Song	465
54	RMC8-P17	<i>Development of Construction Material for Covering of Seabed Resources Using Fly Ash</i> H. Shimada, T. Sasaoka, S. Wahyudi, S. Fujita, Y. Yoshida and K. Takahashi	475
55	RMC9-P26	<i>Prediction of Rockburst Potential under High Geo-Stress: Experimental Study</i> S. Vathna, L. Sanghyun and S. Ki-II	483

56	RMC10-P207	<i>Comprehensive Laboratory Study of a Slightly Metamorphosed Limestone</i> L. N. Y. Wong, V. Maruvanchery and N. N. Oo	489
57	RMC11-P122	<i>Considerations on Friction Angles of Planar Rock Surfaces with Different Surface Morphologies from Tilting and Direct Shear Tests</i> Ö. Aydan	497
58	RMC12-P54	<i>Effects of Confining Pressure on Strain Rate-Dependent Deformation and Failure of Kimachi Sandstone</i> K. Amo, Y. Fujii, J. Kodama and D. Fukuda	507
59	OPSS1-P4	<i>Geometry Effect of Open Pit and Underground Mine During</i> E. Widiyanto, R. K. Wattimena, S. Kramadibrata and M. A. Rai	515
60	OPSS2-P31	<i>Slope Failure Behaviour Analysis in Open Pit Coal Mining</i> R. H. Musa and S. Saptono	523
61	OPSS3-P24	<i>Rockfall Mitigation and Slope Stabilization Measures in Open Pit Mines and New Development Measure of Attenuator Systems</i> C. Balg and R. L. Fonseca	533
62	OPSS4-P80	<i>Effects of the Change of Soil pH on Soil Erosion in Indonesian Open-Cut Coal Mine</i> S. Ogata, S. Matsumoto, H. Shimada and T. Sasaoka	543
63	OPSS5-P196	<i>Risk Management of Mining Optimization on the Remaining Coal Reserve based on the Failure Probability Analysis at the Bendili Pit, PT. Kaltim Prima Coal</i> H. Pancamanto, W. Ningrum, C. H. Saputra, B. Sulistyono and S. Kramadibrata	551
64	OPSS6-P210	<i>An Experimental Study of the Planar Sliding of Rock Slopes During Dynamic Loading Under Dry and Immersed Conditions</i> K. Adachi, N. Iwata, R. Kiyota, Y. Takahashi, O. Aydan, N. Tokashiki and T. Ishibashi	561
65	RMC13-P36	<i>Dynamic Tensile Failure of Rocks Subjected to Simulated In situ Stresses</i> K. Xia, B. Wu, Y. Xu and Y. Guo	571
66	RMC14-P89	<i>Utilization of Geotechnical Logging for Rockmass Characterization (Case Study In Coal Deposit)</i> L. I. Rachmad, D. Nirrambodo, I. Ega and S. Bayu	581
67	RMC15-P188	<i>Fracture Propagation in Layered Sandstones with Varying Saturation</i> W. Timms, P. Cai, B. David, H. Masoumi, N. Melkounian and J. Heo	589
68	RMC16-P151	<i>The Effect of Clay Content on the Strength of Clay-Bearing Rocks</i> A. Sjadat, A. Purba, U. Barito, K. Sulaeman and R. Hasan	599
69	RMC17-P129	<i>Creep Tests on Limestone from Bazda Antique Underground Quarry in Turkey</i> T. Ito, Ö. Aydan, R. Ulusay, C. Ağan and M. Geniş	607
70	RMC18-P131	<i>Field Experimentation of Rock Quality Designation Measurements at Sandstone Mine, Loa Janan Ulu Village, Loa Janan Sub District, Kutai Kartanegara, East Kalimantan</i> F. Adinata, W. Nugroho, C. Sarungallo, C. Manurung and S. Mahardika	617
71	UMOS7-P9	<i>Constitutive Equation for Creep Closure of Shaft and Borehole in Potash Layers with Varying Carnallite Contents</i> N. Wilalak and K. Fuenkajorn	623

72	UMOS8-P182	<i>Damage Analysis at Drawpoint in Panel 1E, Panel 1F, Panel 1G and Panel 1H DOZ Underground Mine Area PT Freeport Indonesia</i> C. Andrianto, A. Sjadat, A. Kurniawan, A. Mulyadi and A. Ginting	631
73	UMOS9-P12	<i>A Comparative Performance Analysis of Wireless Sensor Network Topologies for Underground Spaces Monitoring</i> M. A. Moridi, M. Sharifzadeh, Y. Kawamura and E. K. Chanda	641
74	UMOS10-P101	<i>Sill Pillar Application for Crown Pillar Recovery Optimization in Overhand Cut and Fill Underground Mine</i> T. Karian, H. Shimada, T. Sasaoka, S. Wahyudi and B. Sulistianto	651
75	UMOS11-P67	<i>Application of CMRR Classification System to Determine Rock Mass Design Parameters in Underground Coal Mines</i> A. Taheri and M. Guardado	661
76	UMOS12-P73	<i>Prediction of Disc Cutter Wear for a Hard Rock TBM Based on Improved Energy Method and Empirical Analysis</i> F. Zhao, Y. Xue and Z. Diao	671
77	EN9-P167	<i>Influence of Injection Rate and Viscosity on Hydraulic fracturing Behaviour of Granite</i> S. G. Jung, M. B. Diaz, L. Zhuang, K. Y. Kim, H. S. Shin, S. Yeom and J. H. Jung	681
78	EN10-P169	<i>Rock Mechanical Properties Modeling Of "GE" Exploration Wells to Prevent Wellbore Instability</i> D. R. Febriansanu, E. Andhini, B. S. Pambudi, N. T. Santoso and A. H. Lukman	689
79	EN11-P100	<i>Reservoir Simulation of Part of Yurubcheno-Tokhoms koye Oil Field Based on Geological Geomechanical Model</i> Y. A. Kashnikov, S. G. Ashikhmin, D. V. Shustov, S. Y. Yakimov and A. E. Kukhtinskii	699
80	EN12-P149	<i>Development of Source Locating Technique and its Validation</i> S. Choi and S. Jeon	707
81	EN13-P139	<i>Model-Based Quantitative Rock Mass Classification with Geophysical Data</i> T. Takahashi	715
82	EN14-P43	<i>Wellbore Stability Analysis during Underbalanced Drilling of Horizontal Wells Using Mogi-Coulomb Criterion</i> J. Zhou, S. He, W. Wang, X. Luo and Y. Zhang	723
83	IN9-P48	<i>Engineering Geological Investigations and Rock Mass Characterization for a Road Tunnel in the Himalayas</i> R. Bhasin, A. Aarset and T. Pabst	731
84	IN10-P135	<i>Coupling Analysis of Rock Mass and Water for Debris Flow on a Rock Slope by DDA (Discontinuous Deformation Analysis) and MPS (Moving Particle Simulation) Method</i> M. Kuno, S. Miki, Y. Ohnishi and T. Sasaki	739
85	IN11-P33	<i>Experimental Study of Sodium Silicate Grouting Material: Characterization and Mechanical Performances</i> R. S. Putranto, H. Shimada, T. Sasaoka, S. Wahyudi, S. Fujita and Y. Kanemasu	749
86	IN12-P186	<i>Hydraulic Fracture Testing for the Xe Pian - Xe Namnoy HPP</i> R.J. Longden and G. Klee	757

87	IN13-P82	<i>Application of Chain Conveyor Cutter (CCC) method to Construction of Ocean Disposal Sites</i> S. Matsumoto, H. Shimada, T. Sasaoka, S. Ikuta and T. Sakiyama	767
88	IN14-P99	<i>Slope Stability Analysis Considering the Variability of Hydraulic Conductivity under Rainfall Infiltration. Case Study: Sangun Mountainous, Fukuoka Prefecture, Japan</i> H. Pachri, Y. Mitani and H. Ikemi	775
Poster Presentation			
1	PO1-P13	<i>Uniaxial Compressive Strength Effects on Abrasive Waterjet Cutting Performance for Rock Excavation</i> TM. Oh, ES. Park, GC. Cho and GW. Joo	783
2	PO2-P32	<i>Determining the Effect of Texture Coefficient on Performance of Diamond Wire Machines</i> D. Tumas, S. Er, E. Avunduk, M. Basyigit, H. Copur and C. Balci	789
3	PO3-P61	<i>Rock Strength Characteristics of Warukin Formation (KIDECO) and Field Applications</i> HY. Kim, K. Setiadi and GN. Park	797
4	PO4-P74	<i>A 3D Distinct Element-Based Model for Deformation and Failure of Rock</i> T. Nishimura, K. Fumimura, M. Kohno and D. Mitsuhashi	807
5	PO5-P88	<i>Evolution of Rock Permeability Evaluated by Coupled Thermal-Hydraulic-Mechanical-Chemical Model</i> H. Yasuhara, N. Kinoshita and K. Kishida	817
6	PO6-P108	<i>Correlating Fracture Properties of Saturated Sedimentary Rocks with Compressive Strength</i> D. G. Roy, T. N. Singh and J. Kodikara	823
7	PO7-P111	<i>Physical and Mechanical Properties of Artificial Rock based on Clay Mineral Content and Type</i> M. Kohno, Y. Takehara and T. Nishimura	831
8	PO8-P112	<i>Experimentation of Estimation Rippability on Jointed Rock Mass</i> G. T. V. Herman, H. Hasan, F. D. Mustika and J. Suhadha	839
9	PO9-P137	<i>Stability Assessment of Fractured Natural Slope along a Shore Road using Key Block Analysis and Discontinuous Deformation Analysis (DDA)</i> T. Nakai, Y. Maruki, K. Fukutsuka, T. Nishiumi and Y. Ohnishi	845
10	PO10-P162	<i>Applicability of NMM-DDA with Node-based Element for the Bearing Capacity of Cohesive-frictional Ground</i> R. Hashimoto, T. Koyama and M. Kikumoto	855
11	PO11-P235	<i>Coupled Hydro-Mechanical Analysis for Viscous Grout Injection in a Rock Joint</i> JW. Lee, AR. Kim, HM. Kim, M. Yazdani and ES. Park	863
12	PO12-P234	<i>Impact of Well Orientation on the Geomechanical Stability of Aquifer System during CO₂ Injection</i> AR. Kim, JW. Lee and HM. Kim	871
13	PO13-P38	<i>Dependence of Dynamic Properties of Longyou Sandstone on Heat-Treatment Temperature and Loading Rate</i> W. Yao, Y. Xu and K. Xia	879
14	PO14-P50	<i>Stress Dependency of Permeability in High Temperature Fractured Granite</i> N. Watanabe, M. Egawa and K. Sakaguchi	887

15	PO15-P58	<i>Correction Model for Strength Parameters of a Multistage Triaxial Compression Test on Sandstone</i> X. Shi, L. Liu, Y. Meng, S. Mao, W. Wang, J. Wu and C. Wen	895
16	PO16-P66	<i>Hydraulic Fracturing in Inada Granite under Brittle-Ductile Condition</i> M. Egawa, N. Watanabe and K. Sakaguchi	905
17	PO17-P75	<i>Effect of Difficult Ground Conditions on Double Shield TBM Performance</i> E. Avunduk, A. S. Mamaghani and D. Tumac	915
18	PO18-P81	<i>Numerical Simulation on Shear Behavior of Rock Discontinuities under Various Thermal, Hydraulic and Mechanical Conditions</i> T. Kim, S. Jeon and SB. Choi	925
19	PO19-P91	<i>Integrated Evaluation of In-situ Stress Measurement and Borehole Scanning Result for Estimation of Rock Stress State in Pohang Basin</i> S. H. Bae, S. Jeon, KB. Min and J.S. Kim	933
20	PO20-P116	<i>Application of Rock Mass Quality Rating (RMQR) and Rock Mass Classification System at Andesite Open Pit Mining in West Sumatera</i> M. A. Fikri, and Y. Azzuhry	941
21	PO21-P118	<i>Strain and Strength of Saturated and Dried Rock Samples Under a Freeze-Thaw Cycle</i> R. A. Sudisman, T. Yamabe and M. Osada	951
22	PO22-P128	<i>Unloading Crack of Hard Rock and its Restraining Support Method: Case Study in a Large Underground Cavern with High Geostress Condition</i> Q. Jiang, YL. Fan, XT. Feng, Y. Li, W. He and GF. Liu	961
23	PO23-P141	<i>Study a Correlation of Ultrasonic Wave and Numerical Modeling under Biaxial Load Test in Laboratory Scale</i> Herman, N.P. Widodo, I. Arif and B. Sulistianto	969
24	PO24-P144	<i>Study of Physical and Numerical Model in Determination of Fracture Toughness Mode I Using Three Point Bending and Brazilian Test for Andesite, Limestone and Cement Paste</i> S. Aqla, N.P. Widodo and M.A. Rai	977
25	PO25-P145	<i>A Study on The Extraction of Slope Surface Orientation using LIDAR with Respect to Triangulation Method and Sampling on The Point Cloud</i> S. Lee and S. Jeon	987
26	PO26-P163	<i>Development of Hydraulic Stimulation Simulator for Comprehensive EGS Stimulation Design</i> S. Park, L. Xie, H. Yoo, KI. Kim and KB. Min	995
27	PO27-P201	<i>Fluid Flow Simulation through 3-D Discrete Fracture Networks</i> N. Huang, Y. Jiang, R. Liu and B. Li	1005
28	PO28-P25	<i>Estimation of Rock Mass Stress State Based on Convergence Measurement during Gallery Excavation</i> K. Aoyagi, M. Nago, K. Kamemura and K. Sugawara	1013
29	PO29-P39	<i>Anisotropic Distribution of the Rock Mass Resistant Coefficient around a Circular Tunnel in Jointed Rock Masses</i> H. Tu and C. Qiao	1023

30	PO30-P47	<i>Travel Distance Prediction Analysis for Work Safety Distance On The Potential of Mining Slope Failure in Indonesia</i> R. R. Putra and Y. Azzuhry	1033
31	PO31-P72	<i>Numerical Simulation of Transient Heat Conduction in Anisotropic Medium Based on SPH-FDM Coupling Algorithm</i> X. Tao, C. Peipei , B. Bing and Z. Chenggang	1041
32	PO32-P90	<i>3-D Analysis of Time-dependent Behavior of Tunnel Crossing Weak Rock Formation</i> J. Kodama, S. Tabata, D. Fukuda, Y. Fujii, H. Murayama, H. Niwa and A. Sainoki	1047
33	PO33-P109	<i>Implementation of Study Rockfall Hazard Rating System (RHRS) Method for Slope Stability Analysis at Samarinda Seberang District, East Kalimantan, Indonesia</i> N. Rohmah, T. Trides, M. Fitra, G. I. Santoso and Suhbajir	1055
34	PO34-P147	<i>Experimental Study on the Measurements of Electrical Impedance and P-wave Velocity of a Low Permeable Rock Core during the Displacement of Saturated Brine by CO2 Injection</i> H. Honda, M. Imasato, S. Takaki, H. Ikemi, K. Kitamura and Y. Mitani	1063
35	PO35-P165	<i>Rock Slopes Stability Evaluation Based on Comparison Empirical Methods “Slope Mass Rating” and Analytical Method at Discontinuities Rock Mass Condition (Case Study at Sandstone Mines, Tani Aman Village, Loa Janan Sub District, Samarinda, East Kalimantan, Indonesia)</i> T. Trides, J. P. Londa and P. Laksono	1069
36	PO36-P215	<i>Stick-Slip Behavior of Rock Discontinuities and Its Implications in the Estimation of Strong Motions during Earthquakes</i> N. Iwata, K. Adachi, Y. Takahashi and Ö. Aydan	1079
37	PO37-P37	<i>A Review of the Non-destructive Testing Methods to Evaluate Tunnel Lining Integrity</i> Y. Gao and Y. Jiang	1089
38	PO38-P96	<i>Analysis of a Geothermal Double-well System Based on Numerical Simulation and In-situ Tracer Test</i> S. Luo, E. Song and Z. Zhao	1097
39	PO39-P191	<i>Correlation between Full Core and Half Core Specimen for Point Load Index in Poboya River Reef Gold-Silver Deposit</i> D. Kusumanto, A. B. Pramusi, C. Nursetyo and A. Rahman	1107
40	PO40-P226	<i>Prediction of Rock Failure Strength Based on Comparison Between Water Surface and Finite Element Analysis (FEA) Steady State</i> Y. Sugianto, M. A. Azizi and H. Saliman	1115
41	PO41-P132	<i>Numerical and Analytical Study on the Plane Elastic Waves Propagating in Layered Saturated Porous Half-Space</i> P. Li and E. Song	1123
42	PO42-P214	<i>Elasto-Plastic Analysis of Deformations in Twin Interacting Horse Shoe Tunnels</i> I. A. Khan, K. Venkatesh and R. K. Srivastava	1133
43	PO43-P11	<i>Core Disking Analysis to Characterize Potential High Horizontal Stress in Open Pit Mine</i> J. W. Tu’u, I. Arif, N. P. Widodo and E. Widijanto	1141

44	PO44-P3	<i>Plastic Zone Prediction Using Finite Element Method on Cikoneng Decline Tunnel at PT. Cibaliung Sumberdaya</i> B. P. Putra, B. Sulistianto, G. M. Simangunsong and N. P. Widodo	1149
Proceeding Only			
1	PR1-P7	<i>Evaluation of Shear Strength of Rock Discontinuities on Direct Shear Test Result of Sawtooth Joint Models</i> Kartini, Jackie, G. M. Simangunsong and B. Sulistianto	1159
2	PR2-P156	<i>Measurement of Blast Fragmentation Using Image Processing Analysis 3D Photogrammetry</i> S. Hidayat, G. M. Simangunsong and D. Suwardhi	1167
3	PR3-P124	<i>Application of Clustering System to Analyze Geological, Geotechnical and Hydrogeological Data Base according to HC-System Approach</i> L. E. Widodo, T. A. Cahyadi, S. Notosiswoyo and E. Widijanto	1175
4	PR4-P30	<i>Experimental Investigation of Contact Area on Wave Propagation and Closure Deformation of Rock Joints</i> N. N. Li, J. C. Li, L. F. Rong and H. B. Li	1185
5	PR5-P105	<i>The Development of Wetmuck Classification as a Tool for Controlling and Monitoring Mudrush Hazard (PT Freeport Indonesia Wetmuck Case History - Part I)</i> L. I. Rachmad, A. Sjadat and A. P. Ginting	1193
6	PR6-P224	<i>A Comparison on Rock Slope Stability Analysis of Phu kam Copper-Gold Open Pit Mine, Laos PDR by Limit Equilibrium, Finite Element and Finite Difference Methods</i> K. Manivang, G. M. Simangunsong and R. K. Wattimena	1199

LEGEND	
EN	: ENERGY
IN	: INFRASTRUCTURE
RMC	: ROCKMASS CHARACTERIZATION
CMNM	: CONSTITUTIVE MODELS & NUMERICAL MODELLING
RE	: ROCK EXCAVATION
UMOS	: UNDERGROUND MINE OPENING STABILITY
OPSS	: OPENPIT SLOPE STABILITY

Evaluation of Ground Support by Rock Mass Index and Finite Element Method Numerical Modelling PT Cibaliung Sumberdaya Banten

A. Adhareza^{a*}, S. Saptono^a and B. D. Nagara^a

^a *Mining Engineering, UPN "Veteran" Yogyakarta*

*adhareza.adriel@gmail.com (*corresponding author's E-mail*)

Abstract

PT Cibaliung Sumberdaya is one of gold mining company which using cut and fill method for the underground mining system. In underground mining system, all activity doing in ground from surface. The common problem in underground mining activity is the instability of tunnel. Thus, the corrective action needed is evaluate the ground support system itself.

System of ground support certainly requires an analysis from a safety and economic part. Ground support system should be revised refer to mining progress or based on emerging technology in mining area. The evaluation aims to update the primary ground support system in mining which applied by recommendation of Geotechnical Unit, Dept. Quality Control, PT Cibaliung Sumberdaya classified by Rock Mass Rating (RMR) with the new ground support system classified by Rock Mass index (RMi) ones. The meaning of evaluation is to evaluate from a ground support quantity aspect (total split set requirement and thickness of shotcrete) and ground support effective aspect to gain a high safety value. Manual calculation about safety factor (FK) value, plastic zone, stress distribution surrounding the tunnel also available with added a total displacement and strength factor (SF) value from analysis of numerical calculation finite element method with Phase2 v.07 to ensure the empiric method. Result of research in 3 locations e.g Cikoneng Decline, Cikoneng Xcut 2B level 1125 North, Cikoneng Xcut 4 level 1065 Ore Drive 1 South, evaluation of ground support system by Rock Mass index (RMi) more efficient from support quantity and effective from support utility, also give a high value of safety factor for a tunnel.

Keywords: Underground Mine, Ground Support, Rock Mass Classification, Finite Element

1. Introduction

In geographic, PT Cibaliung Sumberdaya located in end South West of Java and in administrative located in Province of Banten. In astronomic, the location of PT Cibaliung Sumberdaya occur at 6° 30' - 6° 52' S and 102° 02' - 105° 37' E. To go to this location from Jakarta could be reached by car transportation via Jakarta – Serang – Pandeglang – Labuan - Cibaliung route in 6 (six) hour.

The purpose of this research is to evaluate the ground support by RMi with the ground support which applied in PT Cibaliung Sumberdaya and compare with numerical modelling (finite element method) to reach an effective and efficient ground support for the tunnel instability potential in underground mining. The limitation of this research is do in Cikoneng area only and the critical condition of stability (safety factor) calculated by Mohr-Coulomb failure criterion. The rock mass classified with Rock Mass index (RMi) by Arild Palmström (2000) and the numerical modelling was calculated and presented with software Phase2 v.07.

2. Theories (or Experiments)

2.1 Theories

Rock Mass index (RMi) is a classification system based on inherent of the rock mass. Basically, this system combine the compressive strength from the intact rock and the parameter of joint condition.

There are 5 (five) input parameters to classify the rock mass by Rmi system: Uniaxial of compressive strength (c), Volume block (Vb), Joint roughness factor (jR), Joint alteration factor (jA), and Joint continuity factor (jL). The value of Rock Mass index (Rmi) parameters could be shown in Table 1.

Table 1 Value of rock mass index (Rmi) input parameters

Uniaxial compressive strength of intact rock (σ_c)		value in MPa (from lab. tests or assumed from handbook tables)				
Block volume (Vb)		value in m ³ (from observations at site or on drill cores, etc.)				
Joint condition factor (jC)		jC = jR x jL / jA (ratings of jR, jA and jL from the tables below)				
jR (joint roughness factor, which is composed of large scale and small scale undulations, similar to Jr in the Q-system)						
(The ratings in bold italic are similar to Jr)		Large scale waviness of joint plane				
		Planar	Slightly undulating	Undulating	Strongly undulating	Stepped or interlocking
Small scale smoothness of joint surface	Very rough	2	3	4	6	6
	Rough	1.5	2	3	4.5	6
	Smooth	1	1.5	2	3	4
	Polished or slickensided ^{*)}	0.5	1	1.5	2	3
For filled joints jR = 1 For irregular joints a rating of jR = 6 is suggested						
^{*)} For slickensided surfaces the ratings apply to possible movement along the lineations						
jA (joint alteration factor, which ratings are based on Ja in the Q-system)						
Contact between joint walls	CLEAN JOINTS:	Healed or welded joints	filling of quartz, epidote, etc.	jA = 0.75		
		Fresh joint walls	no coating or filling, except from staining (rust)	1		
		Altered joint walls	- one grade higher alteration than the rock - two grades higher alteration than the rock	2 4		
	COATING or THIN FILLING OF:	Frictional materials	sand, silt calcite, etc. without content of clay	3		
Purity or no well contact	THICK FILLING OF:	Cohesive materials	clay, chlorite, talc, etc.	4		
		Frictional materials	sand, silt calcite, etc. (non-softening)	jA = 4 8		
		Hard, cohesive materials	clay, chlorite, talc, etc.	6 5 - 10		
		Soft, cohesive materials	clay, chlorite, talc, etc.	8 12		
Swelling clay materials	material exhibits swelling properties	8 - 12 13 - 20				
				Thin filling (< 5 mm)	Thick filling	
jL (joint size factor, which is composed of the length and continuity of the joint)				Continuous joints	Discont. joints^{*)}	
Bedding or foliation partings		length < 0.5 m	jL = 3		jL = 6	
Joints		with length 0.1 - 1 m	2		4	
		with length 1 - 10 m	1		2	
		with length 10 - 30 m	0.75		1.5	
(Filled) joint, seam or shear ^{**)}		length > 30 m	0.5		1	
^{*)} Discontinuous joints end in massive rock ^{**)} Often a singularity and should in these cases be treated separately						

There is a formula to define the value of Rmi based on the jointed rock, as shown in Eq.1

$$Rmi = \sigma_c \cdot JP \tag{1}$$

where σ_c = uniaxial compressive strength based on the UCS/PLi test
JP = joint parameter value

To define the value of joint parameter (JP) can be found

$$JP = \sigma_c \cdot 0.2 \sqrt{jC} \cdot Vb^D \tag{2}$$

where jC = joint condition factor
Vb = block of rock volumes (m³)
Db = diameter of rock block (m³)

$$Db = \sqrt[3]{Vb} \tag{3}$$

$$D = 0.37 \cdot jC^{-0.2}$$

Rmi is obtained a value of Rmi on tunnel or hole openings are examined. There are 6 (six) class on the value of the Rmi. For more details can be seen in the following table

Table 2 Rock mass index (Rmi) classification

Rmi =	100 - 40	Very high
Rmi =	40 - 10	High
Rmi =	10 - 1	Moderate
Rmi =	1 - 0.4	Low
Rmi =	0.4 - 0.1	Very low
Rmi =	0.1 - 0.01	Extremely low

Values of the R_{Mi} obtained must be calculated again based on continuity of rock mass factor (CF). Continuity of rock mass factor is a factor of joint continuity. If joint that does not intersect with another joint then it can be said to be of continuity of ground type is massive or highly jointed or particulated (CF < 5 or > 100). If the joint intersect with other joint, then it can be said the continuity of ground type is jointed (CF 5 to 100). The value of the CF was obtained from the following formula

$$CF = Dt(\text{span}) / Db \tag{4}$$

where Dt = tunnel diameter
Db = the diameter of rock blocks

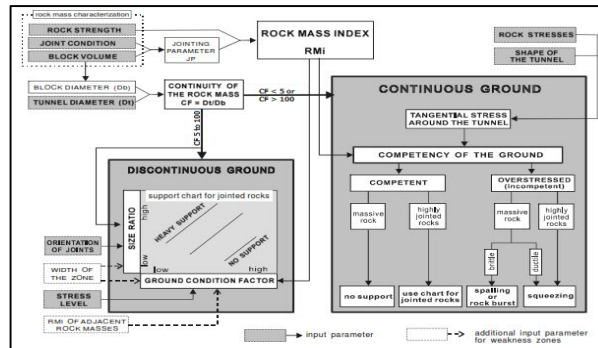


Fig.1 . Rock mass index (R_{Mi}) flowchart

The value of the CF can be grouped into 2 (two) type continuity of the ground. For a continuous ground, the value of the R_{Mi} will be calculated to get the value of the competency of the ground (C_g) based on the value of tangential pressure (σ_θ). And, the value of tangential pressure (σ_θ) around the hole openings of the pressure of rocks either vertically (ρ_v) and horizontal (ρ_h), influence of ground water (ground water), shape, span (W_t), and the diameter of the hole openings (D). For discontinuous ground, the value of the R_{Mi} will be calculated to get the value of the ground condition factor (G_c) based on the stress factor level (SL) and the size ratio (S_r) based on the orientation of the joint. For more details and calculations in determining any needs of the R_{Mi} obtained, it as shown in Figure.1 .

2.2 Experiments

1. Rock Mass Condition and Properties

Mechanical and physical properties of rock mass can be seen in Table 3 as follows:

Table 3 Mechanical & physical properties of rock mass

No	Location	Rock Mass	σ _c (MPa)	GSI	Cohesion (c)	Angle of Friction (°/deg)	Young Modulus (MPa)	Tensile Strength (MPa)
1	Cikoneng Decline	Porphyry Andesite	36.3	34	0.42	40.19	978.61	0.01
2	Cikoneng Xcut 2B level 1125 North	Quartz Vein Breccia	64.5	36	0.25	46.76	1561.60	0.01
		Clay Matrix Breccia – Porphyry Andesite						
3	Cikoneng Xcut 4 level 1065 Ore Drive 1 South	Stockwork –	53.7	33	0.35	37.91	1197.46	0.01
		Clay Matrix Breccia – Quartz Vein						

2. Joint Condition (jC)

Joint Condition (jC) obtained from the calculation of the 3 parameters i.e. joint roughness (JR), joint alteration (jA), and the joint length (jL). For more details can be seen in Table 4 below.

Table 4 Joint condition (jC)

No	Location	Joint Roughness (jR)	Joint Alteration (jA)	Joint Continuity (jL)	Joint Condition (jC)
1	Cikoneng Decline	2 (slightly undulating – rough)	4 (thin filling – clay)	1.5 (10 – 30 m)	0.75
2	Cikoneng Xcut 2B level 1125 North	3 (undulating – rough)	4 (thin filling – clay)	2 (1 – 10 m)	1.5
3	Cikoneng Xcut 4 level 1065 Ore Drive 1 South	3 (undulating – rough)	3 (thin filling – silica)	2 (1 – 10 m)	2

3. Joint Parameters (JP) and the value of the Rock Mass index (RMi)

Joint Parameter is the parameter values obtained from joint based on the calculation of the value of the volume of blocks rocks (Vb), constants D, and joint condition (jC). Based on the value of this JP can be calculated the value of Rock Mass index (RMi) at each location. For more details can be seen in Table 5 as follows.

Table 5 Joint parameter (JP)

No	Location	Joint Condition (jC)	Volume of Block Rocks (Vb)	Konstanta D	Joint Parameter (JP)	RMi Value
1	Cikoneng Decline	0.75	0.200 m ³	0.39	0.090	3.27 (III – moderate)
2	Cikoneng Xcut 2B level 1125 North	1.5	0.070 m ³	0.34	0.099	6.39 (III – moderate)
3	Cikoneng Xcut 4 level 1065 Ore Drive 1 South	2	0.004 m ³	0.3	0.043	2.31 (III – moderate)

4. Continuity Factor (CF)

Cikoneng Decline tunnel diameter i.e. 4.78 m and the value of the Db that is 0.62 m so that the value of the CF gained i.e 8 with the category of discontinuous ground. As for the location of Cikoneng Xcut 2B level 1125 North tunnel diameter i.e. 5.11 m and the value of the Db that is 0.41 m so that the value of CF obtained i.e. 12 with the discontinuous category. Then, for the location of the 1065 level 4 Xcut Cikoneng Ore Drive 1 South has a diameter tunnel i.e 4.32 m and the value of the Db that is 0.16 m so that the value of CF obtained i.e. 27 with the discontinuous category of ground.

5. The Influence Surrounding the Tunnel

Based on the results of the calculations are then obtained the influence of stress level (SL), groundwater (GW), factor of joint set adjustment (Nj), the inclination and orientation on the roof and the wall as follows. (see Table 6).

Table 6 Influence of stress level, groundwater, the inclination and orientation

No	Location	Stress Level (SL)	Ground -water (GW)	Roof Inclination (C_{roof})	Wall Inclination (C_{wall})	Roof Orientation ($C_{o_{roof}}$)	Wall Orientation ($C_{o_{wall}}$)	Factor of Joint Set Adjustment (Nj)
1	Cikoneng Decline	1.50	1	2.80	2.30	1	2	0,50 (6 joint sets)
2	Cikoneng Xcut 2B level 1125 North	1.50	1	2.60	3.30	1	1.50	0,75 (4 joint sets)
3	Cikoneng Xcut 4 level 1065 Ore Drive 1 South	1.50	1	3.60	1.90	1	1.50	1,50 (2 joint sets)

6. Ground Condition (Gc), Size Ratio (Sr), and the Determination of Bolt Length (Lb)

Here are graphs that contain a combination of support quantity needs from Ground Condition (Gc), Size Ratio (Sr) values and bolt length (Lb). (see Table and Figure below).

Table 7 Ground condition (Gc), size ratio (Sr), and bolt length (Lb)

No	Location	Ground Condition (Gc)		Size Ratio (Sr)		Bolt Length (Lb)	
		Roof	Wall	Roof	Wall	Roof	Wall
1	Cikoneng Decline	14	11	16	26	1.4 m	2.0 m
2	Cikoneng Xcut 2B level 1125 North	25	32	17	25	1.5 m	2.1 m
3	Cikoneng Xcut 4 level 1065 Ore Drive 1 South	12	7	18	27	2.5 m	1.4 m

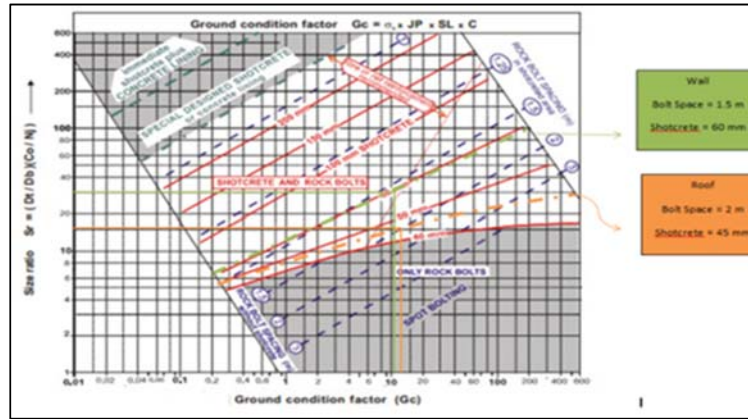


Fig. 2. Cikoneng decline rockbolt and shotcrete support combinations

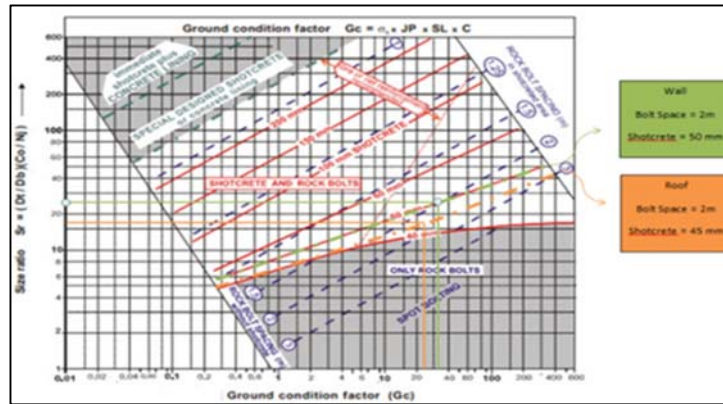


Fig. 3. Cikoneng xcut 2b level 1125 north rockbolt and shotcrete support combinations

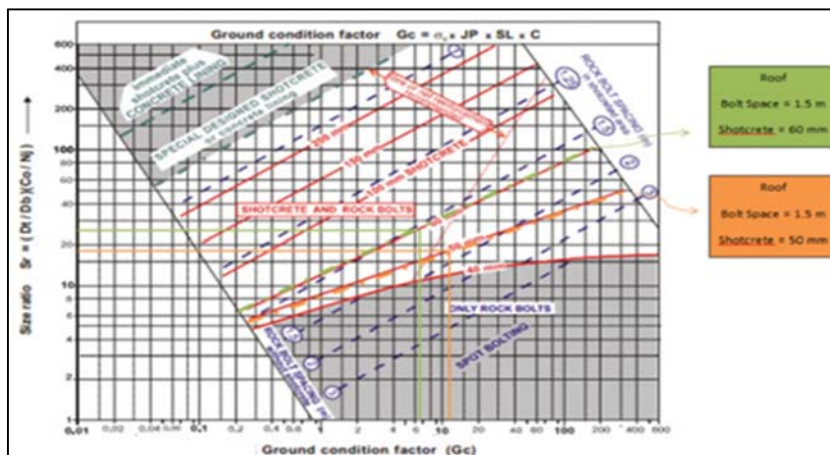


Fig. 4. Cikoneng xcut 4 level 1065 ore drive 1 south rockbolt and shotcrete support combinations

7. Safety Factor, The Rate of Displacement, Distribution of Stress Surrounding the Tunnel, and Plastic Zone

Table 8 Safety factor, the rate of displacement, distribution of stress, and plastic zone

	Cikoneng Decline		Cikoneng Xcut 2B level 1125 North		Cikoneng Xcut 4 level 1065 Ore Drive 1 South		
	Roof	Wall	Roof	Wall	Roof	Wall	
Safety Factor	0.97	1.56 – 1.65	0.61	0.72 – 0.74	0.66	1.28 – 1.39	
Rate of Critical Displacement (V _r)	51.822 x 10 ⁻⁵ mm/day		37.570 x 10 ⁻⁵ mm/day		49.460 x 10 ⁻⁵ mm/day		
Rate of Maximum Displacement (V _r max)	33.273 x 10 ⁻² mm/day		28 x 10 ⁻³ mm/day		61 x 10 ⁻³ mm/day		
Distribution of Stress Surrounding the Tunnel (MPa)	Major Stress (σ ₁)	3.63	1.00	2.80	1.44	1.75	0.78 – 0.86
	Minor Stress (σ ₃)	0.43	0.08 – 0.11	0.34	0.12	0.21	0.14
	Vertical Stress (σ _v)	3.34		1.41		2.98	
	Horizontal Stress (σ _h)	1.04		0.65		0.98	
	Radial Stress (σ _r)	0		0		0	
	Tangential Stress (σ _θ)	7.83	-0.22	3.58	0.54	7.96	-2.02
	Shear Stress (σ _{rθ})	0		0		0	
	Plastic Zone (m)	1.74		1.71		1.61	

3. Result and Discussion

1. Support Requirement

Table 9 Support requirement

No	Location	Rock Mass Value	Rockbolt (Splitset)		Shotcrete Thickness	Additional
			Space	Quantity		
1	Cikoneng Decline	RMi = 3.26	1.5 – 2 m	8 pcs	1 st layer 45 – 60 mm	Forepolling 2.40 m
		RMR = 39	1.20 m	11 pcs	1 st layer 50 mm, 2 nd layer 100mm fibrecrete	
2	Cikoneng Xcut 2B level 1125 North	RMi = 6.37	2 m	7 pcs	1 st layer 45 -50 mm	
		RMR = 41	1.50 m	9 pcs	1 st layer 50 mm	
3	Cikoneng Xcut 4 level 1065 Ore Drive 1 South	RMi = 2.30	1.50 m	8 pcs	1 st layer fibrecrete 50 – 60mm	Forepolling 2.40 m
		RMR = 38	1.10	11 pcs	1 st layer 50 mm, 2 nd layer 100mm fibrecrete	

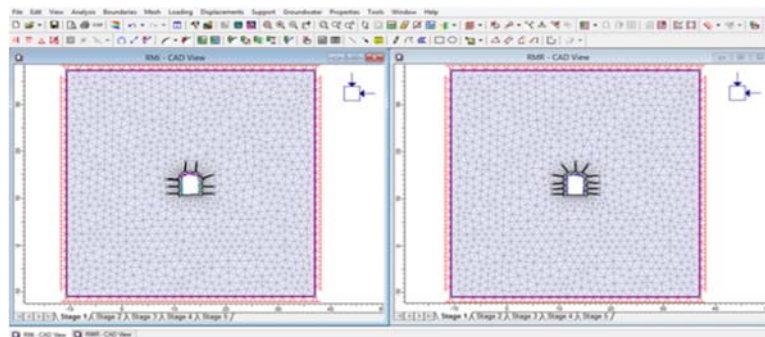


Fig. 5.Cikoneng decline support quantity

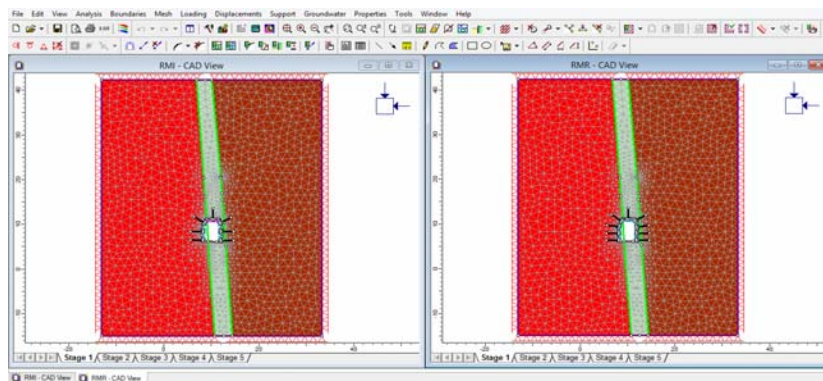


Fig. 6.Cikoneng xcut 2b level 1125 north support quantity

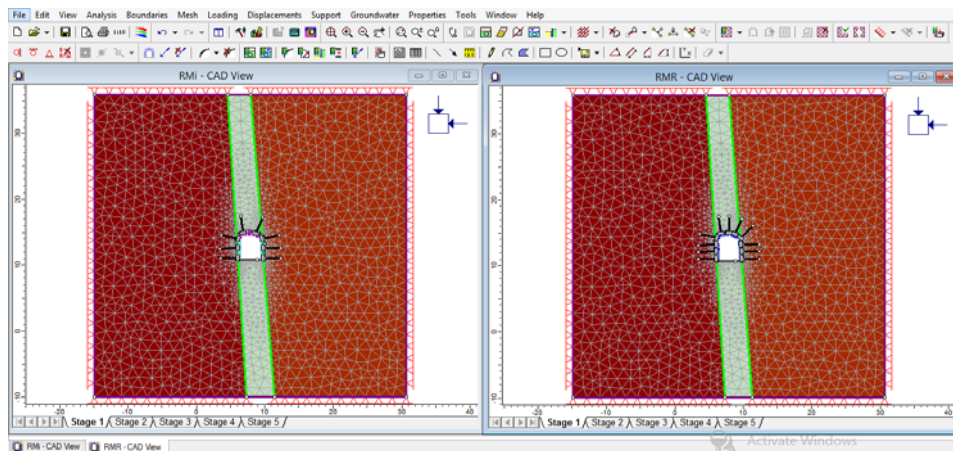


Fig. 7. Cikoneng xcut 4 level 1065 ore drive 1 south support quantity

2. Strength Factor

Table 10 Strength factor value

No	Location	Support Design by Rock Mass Classification	Strength Factor (SF) Value			
			No Support		Supported	
			Roof	Wall	Roof	Wall
1	Cikoneng Decline	RMi	0.95	0.95 – 1.26	1.89	3.16 – 4.11
		RMR			1.89	2.53 – 3.79
2	Cikoneng Xcut 2B level 1125 North	RMi	0.95	0.95	0.95 – 1.58	1.58 – 2.21
		RMR			0.95 – 1.26	1.58 – 2.21
3	Cikoneng Xcut 4 level 1065 Ore Drive 1 South	RMi	0.95	1.26 – 1.89	1.58	3.79 – 4.74
		RMR			1.58	3.47 – 4.79

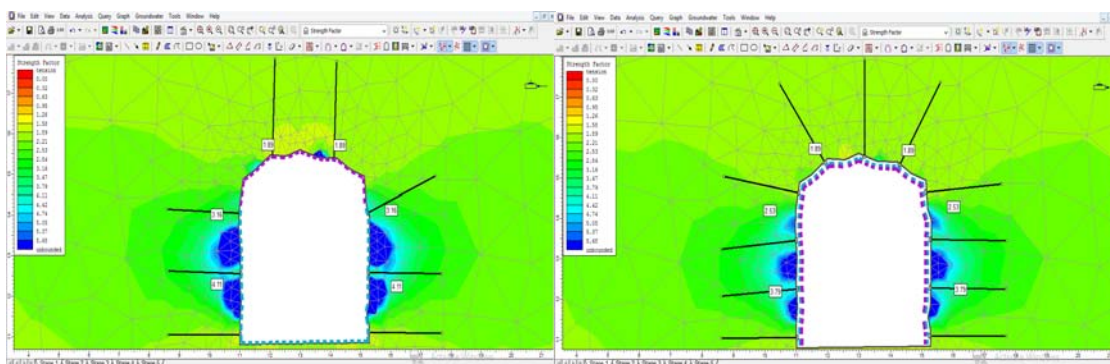


Fig. 8. Cikoneng decline strength factor value

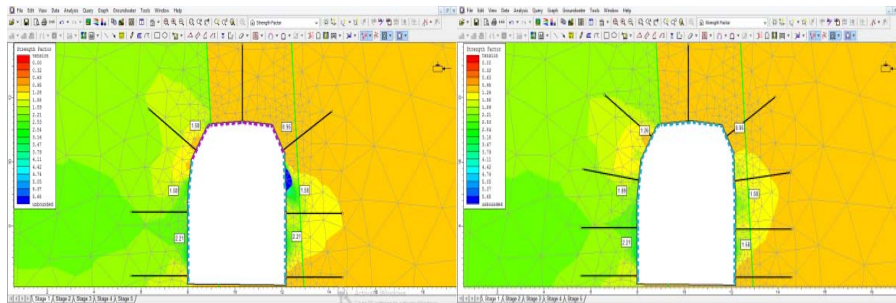


Fig. 9. Cikoneng xcut 2b level 1125 north strength factor value

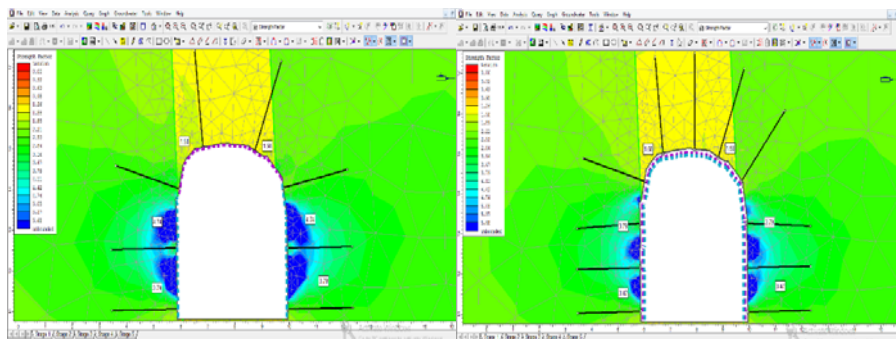


Fig. 10. Cikoneng xcut 4 level 1065 ore drive 1 south strength factor value

4. Conclusions

- Quantity of rockbolt requirement (splitset) and thickness of shotcrete on the support modelling which classified base on classification of Rock Mass index (RMI) fewer in number of splitset and much thinner in shotcrete also do not require fibrecrete nor forepolling.
- In general review from support requirements and strength factor value, RMI support design modeling is more effective in support quantity terms as well as efficient in terms of the needs of support.

Acknowledgement

The author would like to thanks for the valuable opportunity to participate in 9th ARMS.

References

- Palmström, A., 1995, *RMI – A Rock Mass Characterization System for Rock Engineering Purposes* (Master's thesis), Retrieved from Norwegian Geotechnical Institute, Norway.
- Palmström, A., 1995, Recent Development in Rock Support Estimates by the RMI, *Journal of Rock Mechanics and Tunneling Technology Vol.6 No.1*, Norway.
- Palmström, A., 1995, RMI – a system for characterizing rock mass strength for use in rock engineering, *Journal of Rock Mechanics and Tunneling Technology Vol. 1 No. 2*, Norway.
- Hoek, E. and Brown, E. T., 1982, *Underground Excavation in Rock*, Institution of Mining and Metallurgy, London.